ACS APPLIED MATERIALS & INTERFACES

Research Article

www.acsami.org

Stable, High Voltage $Li_{0.85}Ni_{0.46}Cu_{0.1}Mn_{1.49}O_4$ Spinel Cathode in a Lithium-Ion Battery Using a Conversion-Type CuO Anode

Roberta Verrelli,[†] Bruno Scrosati,[‡,§] Yang-Kook Sun,[§,⊥] and Jusef Hassoun*[,†]

[†]Chemistry Department, Sapienza, University of Rome, 00185, Rome, Italy

[‡]Italian Institute of Technology, 16163 Genova, Italy

[§]King Abdulaziz University, Chemistry Department, Jeddah 22254, Saudi Arabia

[⊥]Department of Energy Engineering, Hanyang University, Seoul 133-791, South Korea

ABSTRACT: We report in this work a copper-doped $Li_{0.85}Ni_{0.46}Cu_{0.1}Mn_{1.49}O_4$ spinel-structured compound prepared by an easy, two-steps coprecipitation and solid state process and used in a lithium-ion battery in combination with a CuO-based anode. We show that the spinel-type cathode adopts unique morphology, characterized by well-developed, crystalline and aggregated microparticles, that considerably reduces the occurrence of side reactions. This cathode material can operate in a lithium cell at voltages as high as 5.3 V without sign of electrolyte decomposition, delivering a capacity of about 100 mA h g^{-1} with high retention and high Coulombic efficiency over prolonged cycling. The combination of the $Li_{0.85}Ni_{0.46}Cu_{0.1}Mn_{1.49}O_4$ cathode with a conversion-type, CuO−MCMB anode results in a new type of lithium ion battery characterized by a voltage value of 3.4 V, a stable capacity of 100 mA h g^{-1} and a high Coulombic efficiency (exceeding 95%). Expected low cost, safety, and environmental compatibility are additional advantages of the lithium-ion cell reported here.

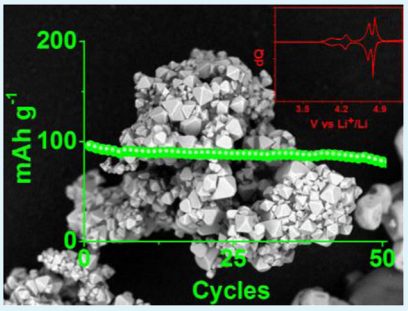

KEYWORDS: *$Li_{0.85}Ni_{0.46}Cu_{0.1}Mn_{1.49}O_4$, high-voltage cathode, spinel-structure, CuO anode, lithium-ion battery*

1. INTRODUCTION

The emerging hybrid and electric automotive market, as well as the development of alternative energy plants, call for new energy storage systems with high performance in terms of efficiency, cost, power, and safety.[1−3] Lithium ion batteries, namely the power sources of choice for consumer electronics, appeared as the most suitable candidates to meet the goal. Substantial progress of the present technology, however, is needed to upgrade lithium batteries to the level requested for proper vehicle operation. It is now well ascertained that a significant breakthrough in this field may be achieved only by the development of electrode materials assuring performance higher than those of the state-of-art.

Viable cathodes alternatives to conventional $LiCoO_2$ are lithium manganese oxide spinel, $LiMn_2O_4$, and its doped compounds, e.g., $LiMn_{2-x}M_xO_4$ with M = Ni, Cu, Fe, and Cr, since they are characterized by higher working voltage, lower cost, and improved environmental sustainability.[4−6] The influence of metal doping on the electrochemical performances of spinel electrodes in lithium cells, both in terms of delivered capacity and cycling stability, has been in fact well-known: a classical example is the nickel-doped $LiNi_{0.5}Mn_{1.5}O_4$ spinel that cycles in lithium cells with a high 4.8 V voltage, combined with a good capacity in the range of 120 mAh g^{-1}.[7−11]

Few examples of multiple doping of lithium manganese oxide electrodes are available in the literature. A first example is a nickel-substituted $LiNi_xCu_{0.5-x}Mn_{1.5}O_4$ ($0 \le x \le 5$) compound reported in 1999 by Ein-Eli et al.[12] More recently, Liu and Manthiram[13] investigated an iron-doped $LiNi_{0.42}Fe_{0.08}Mn_{1.5}O_4$. Moreover, Wang at al.[14] reported a ruthenium-doped $LiNi_{0.4}Ru_{0.05}Mn_{1.5}O_4$ phase. All these materials provided good performance when tested as electrodes in lithium cells, delivering capacity values of the order of 100 mAh g^{-1}, high rates, and good cycle life. However, to our knowledge, a copper-doped material safely operating at voltages higher than 5 V has not been reported so far. Previous similar compounds were in fact prepared with particle size reduced to the nano dimension, a morphology that, if from one side enhances the rate of the electrode, from the other increases its reactivity toward the electrolyte, with resulting limitation in the operating voltage.

A remaining issue for this high voltage spinel is in its poor compatibility with the electrolyte, especially at the end of the charging process. It is therefore of particular importance to develop materials with optimized morphology in terms of particle size and of tap density, such as to achieve the best condition for controlling the electrode stability.[15] Moving from nano- to macrometric particle size may greatly reduce the reactivity of the electrode. Following this approach, we report in this work the synthesis and characterization of a copper-doped, micrometric particle size $Li_{0.85}Ni_{0.46}Cu_{0.1}Mn_{1.49}O_4$ spinel. We show that this material can reversibly cycle in a

Received: January 23, 2014
Accepted: March 10, 2014
Published: March 10, 2014

lithium cell with a charge voltage cutoff higher than 5 V, with a good capacity and, particularly, with no sign of degradation of the electrolyte. Furthermore, we show that this improved spinel may be successfully used as cathode in a new configuration, lithium-ion battery using a CuO−MCMB composite anode. The battery operates for over 50 cycles at an average voltage of 3.4 V and a stable capacity of 100 mAh g^{-1}.

2. RESULTS AND DISCUSSION

2.1. $Li_{0.85}Ni_{0.46}Cu_{0.1}Mn_{1.49}O_4$ Electrode. Figure 1 shows the X-ray diffraction (XRD) pattern of the synthesized sample,

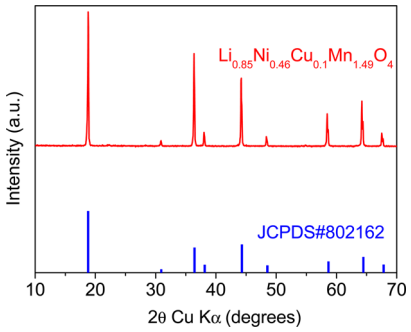

Figure 1. XRD pattern of the $Li_{0.85}Ni_{0.46}Cu_{0.1}Mn_{1.49}O_4$ phase (red curve) and characteristic signals of the $Fd\bar{3}m$ $LiNi_{0.5}Mn_{1.5}O_4$ phase.

described by the molecular formula $Li_{0.85}Ni_{0.46}Cu_{0.1}Mn_{1.49}O_4$. This phase displays a crystalline, cubic, face-centered spinel structure with $Fd\bar{3}m$ space group. All the characteristic signals of the spinel phase (JCPDS: no. 802162) are detected in the XRD pattern, with no signs of impurities.

By Rietveld refinement of diffraction data, we determined that the $Li_{0.85}Ni_{0.46}Cu_{0.1}Mn_{1.49}O_4$ phase is characterized by a cell parameter of about 8.167 Å, a value slightly different compared with that of the conventional $LiNi_{0.5}Mn_{1.5}O_4$ reference phase (8.1667 Å) and by crystalline domains dimensions equal to 1950 (±50) Å.

The graphical representation of the cubic spinel structure adopted by our material, elaborated using the cell parameter determined by the XRD data analysis, and its morphology, studied by scanning electron microscopy (SEM), are reported in Figure 2. The sample consists of highly crystalline, polyhedrally shaped particles organized in uniform aggregates. The particle size ranges from the micrometric (~5 μm) to the submicrometric (~1 μm) scale, with morphology matching the expected one for spinels annealed at temperature higher than 800 °C,[16,17] as in fact is the synthesis condition for our sample (see the Experimental Section).

Figure 3A shows the potendionamic cycling with galvanostatic acceleration (PCGA) curves performed in a three-

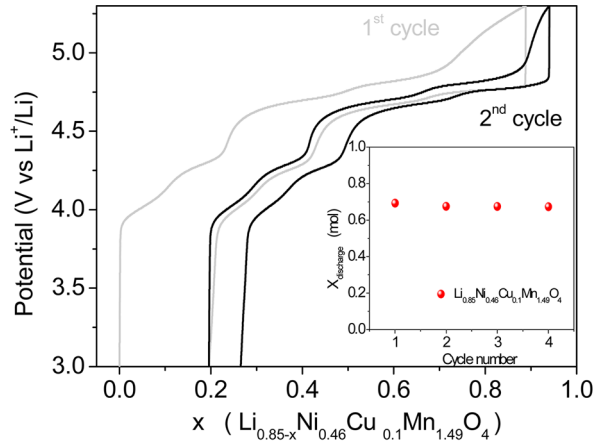

(A)

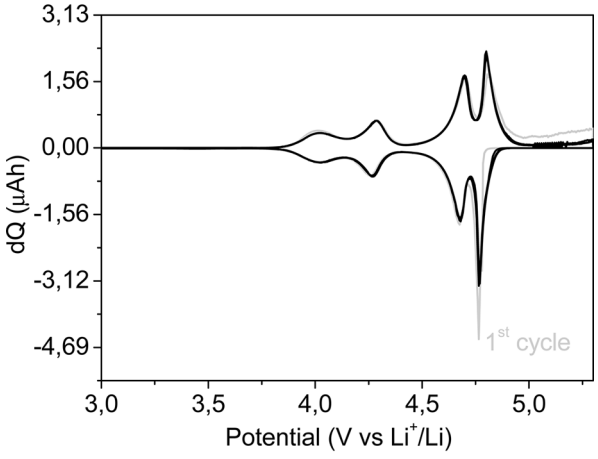

(B)

Figure 3. Potential vs Li^+/Li in function of Li-intercalation degree "x" (A) and incremental capacity versus potential curve during lithium intercalation/deintercalation process. (B) Profiles of the PCGA test of the $Li_{0.85}Ni_{0.46}Cu_{0.1}Mn_{1.49}O_4$ electrode in three electrode configuration lithium cell. (inset) Evolution upon cycling of the equivalents x of Li^+ exchanged during discharge.

electrode lithium cell, within 3−5.3 V limits, in terms of potential evolution of the lithiation−delithiation processes versus Li-intercalation degree (x) upon cycling. We see that the lithium ions intercalated into the electrode spinel structure correspond to 0.68 equivalents during the first discharge and to

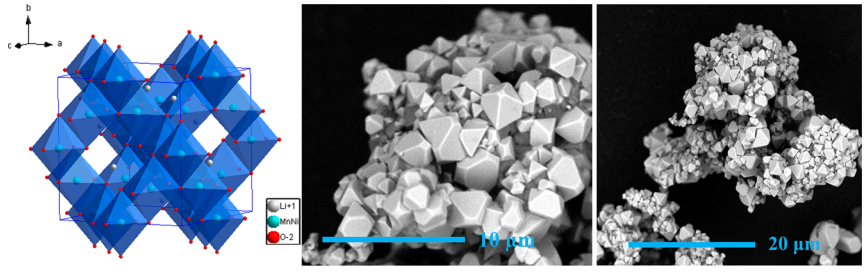

Figure 2. Spinel structure and SEM images of the $Li_{0.85}Ni_{0.46}Cu_{0.1}Mn_{1.49}O_4$ material.

dx.doi.org/10.1021/am500499a | ACS Appl. Mater. Interfaces 2014, 6, 5206−5211

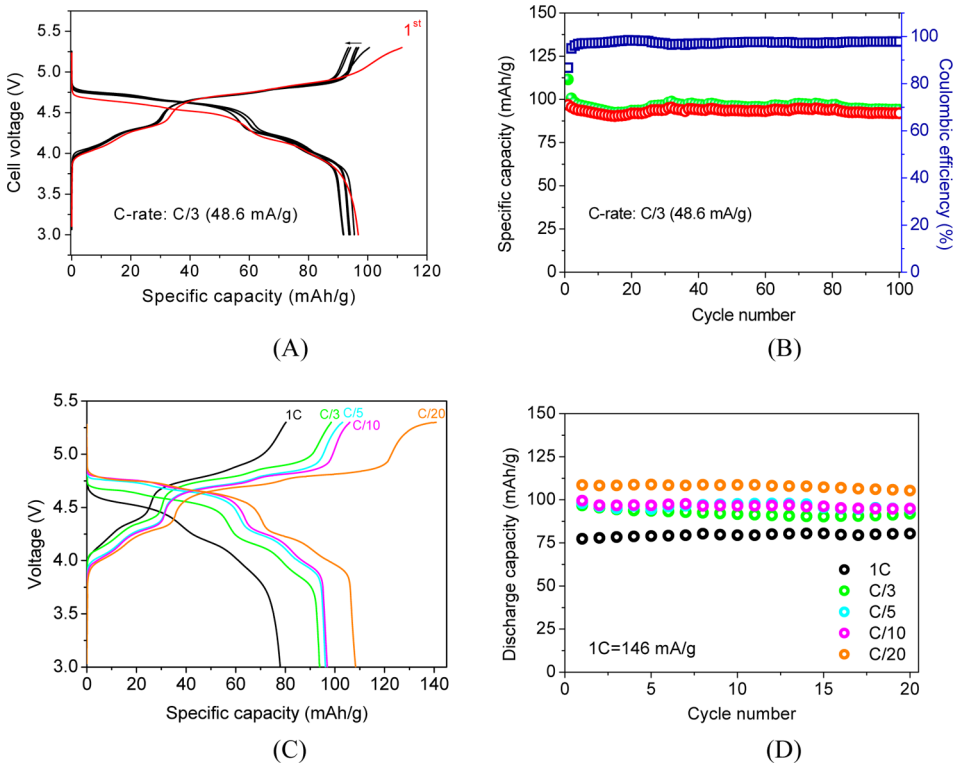

Figure 4. Charge−discharge voltage profiles and specific capacity vs cycle number plot of the Li/1 M $LiPF_6$ PC/$Li_{0.85}Ni_{0.46}Cu_{0.1}Mn_{1.49}O_4$ cell at C/3 rate (A and B) and at different C-rates (C and D).

0.67 in the following ones; see the red dots in the inset figure (reporting the intercalation degree x versus cycles).

Figure 3B, which shows the incremental charge versus potential profile of the PCGA test performed using the $Li_{0.85}Ni_{0.46}Cu_{0.1}Mn_{1.49}O_4$ electrode, demonstrates quite remarkable response. The electrochemical process evolves in charge (delithiation) with four oxidation peaks, at 4.02, 4.28, 4.69, and 4.79 V, respectively. The high voltage peaks at 4.69 and 4.79 V can be attributed to the Ni^{3+}/ Ni^{2+} and the Ni^{4+}/ Ni^{3+} redox couples, respectively, while the signal at 4.02 V is associated to the Mn^{4+}/ Mn^{3+} redox process.[8,12,17,18] The peak centered at 4.28 V may be most likely assigned to the Cu^{3+}/ Cu^{2+} redox couple, as reported by Chemelewsky and Manthiram.[19] However it cannot be excluded that this peak is due to the shift to higher potential, induced by the presence of Cu dopant, of the ∼4 V signal attributed to lithium extraction from the tetrahedral 8a sites, as reported by Fey et al.[18] and Ein-Eli et al.[20] The occurrence of Ni^{4+}/ Ni^{2+} redox reaction at potential values higher than those typically expected, i.e. 4.69−4.79 V instead of 4.6−4.7 V,[8] can be explained taking into account the contribution of the Cu^{3+}/ Cu^{2+} substituent couple,[12] whose signal is at 4.95 V vs Li^+/Li in $LiCu_{0.5}Mn_{1.5}O_4$. The corresponding peaks, displayed in the reverse discharge (lithiation) curve can be clearly identified at 4.01, 4.27, 4.67, and 4.76 V vs Li^+/Li, respectively. The mirror image of the PCGA anodic and cathodic profiles registered in this PCGA test evidences the fast kinetics of the electrochemical process, which cycles with a full reversibility and with an overpotential as low as about 0.01 V. The low irreversibility detected in the high voltage region of the first cycle can be associated with side reactions at the electrode interface resulting from the formation of the solid electrolyte interface (SEI).[21]

Figure 4A shows the response of the $Li_{0.85}Ni_{0.46}Cu_{0.1}Mn_{1.49}O_4$ electrode in a lithium half-cell in terms of charge discharge voltage profiles in the 3.0−5.3 V voltage range and at a current of 48.6 mA g^{-1}, corresponding to a C/3 rate. Four plateau regions, confirming the peak sequence shown by the PCGA curves (compare Figures 3 and 4A) are displayed. The figure evidence that the presence of Cu dopant accounts for a very low polarization of the electrochemical process, resulting in high Coulombic efficiency upon cycling. In addition, the particular morphology of the cathode, characterized by aggregates of well-crystallized particles with submicrometric dimensions, reduces the electrolyte decomposition kinetics, with consequent very high stability even at voltages as high as 5.3. Moreover it is reported in the literature[19] that the octahedral morphology, coupled with abundance of {111} crystallographic planes on the surface, plays a key role in improving the cycling behavior of the electrode, both in terms of stability and rate capability. The electrode cycles with a remarkable capacity stability of about 100 mAh g^{-1} for over 100 cycles and with a charge−discharge efficiency extending up to 98%. To be noticed that the electrode can be cycled up top 5.3 V without any apparent decomposition of the electrolyte. The slight irreversibility detectable in the first cycle may in fact be attributed to the formation of a passivation (SEI) film on the electrode surface.[21]

The delivered capacity corresponds to 69% of the maximum theoretical value, calculated as 146 mAh g^{-1} by considering the exchange of 1 lithium equivalent per mole. This apparently low practical capacity value can be mainly attributed to two factors: (i) the micrometric aggregated morphology, required to increase the electrode stability that, however, may affect the capacity, in particular at high c-rates and (ii) the lithium content that is lower than one. On the other hand, accepting a

capacity at the still considerable value of 100 mAh g^{-1} for assuring high voltage stability appears to be a satisfactory compromise.

Figures 4C and D show the electrode cycling response at different rates, i.e. 1C, C/3, C/5, C/10, and C/20. The related voltage profiles reveal that the electrode polarization follows the expected trend by decreasing as the C-rate decreases. The capacity varies from about 110 mAh g^{-1}, i.e. 75% of the theoretical value, at C/20 to about 75 mAh g^{-1}, i.e. 53% of the theoretical value, at 1 C.

Figure 5A reports the evolution of the electrochemical impedance Nyquist plots of the $Li_{0.85}Ni_{0.46}Cu_{0.1}Mn_{1.49}O_4$

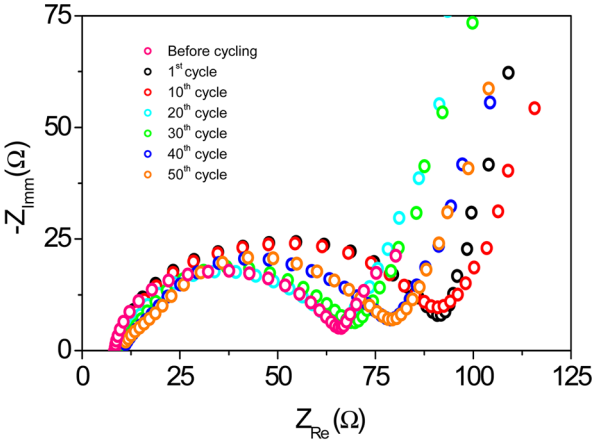

(A)

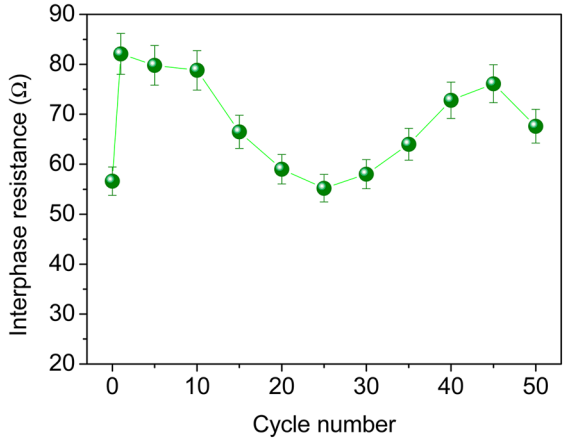

(B)

Figure 5. Nyquist plots of the Li/1 M $LiPF_6$ PC/ $Li_{0.85}Ni_{0.46}Cu_{0.1}Mn_{1.49}O_4$ cell registered at increasing cycle number (A) and corresponding parameters determined by the refinement of the EIS data (B).

electrode upon cycling in lithium half-cell in the set 3.0−5.3 V voltage range. All the spectra, registered at the fully intercalated state of the electrode (3 V vs Li^+/Li), display high-to-medium frequency semicircles that can be interpreted as representatives of interfacial phenomena, such as passivation film formation and charge transfer.[22] Figure 5B, reporting the evolution of the overall interphase resistance upon cycling, evidences a fluctuating trend varying from about 56 Ω at OCV (open circuit voltage before cycling) to about 82 Ω at the end of the first cycle, to then decrease and reincrease between 56 and 76 Ω, in turn reflecting the periodic solid electrolyte interphase (SEI) film formation—dissolution phenomena usually experienced with the progress of the charge/discharge cycles.[23]

2.2. CuO−MCMB/$Li_{0.85}Ni_{0.46}Cu_{0.1}Mn_{1.49}O_4$ Lithium-Ion Battery. The unique characteristics of the $Li_{0.85}Ni_{0.46}Cu_{0.1}Mn_{1.49}O_4$ electrode, including the stability of the electrode/electrolyte interphase upon cycling (see Figure 5) and the suitability to operate at high voltages with good electrochemical performances (see Figures 3 and 4), pose it as a very promising cathode material for advanced lithium ion batteries. To confirm this expectance, a full battery combining $Li_{0.85}Ni_{0.46}Cu_{0.1}Mn_{1.49}O_4$ with a CuO−MCMB composite anode was assembled and tested. The selected anode operates with very good electrochemical performance as demonstrated in a previous work.[24] It is therefore expected that its combination with $Li_{0.85}Ni_{0.46}Cu_{0.1}Mn_{1.49}O_4$ can indeed give rise to a quite valid lithium ion battery operating on the basis of the process:

$$CuO + Li_{0.85}Ni_{0.46}Cu_{0.1}Mn_{1.49}O_4 = Li_xCuO + Li_{(0.85-x)}Ni_{0.46}Cu_{0.1}Mn_{1.49}O_4 \quad (1)$$

Figure 6A shows the electrochemical profiles of the two single electrodes separately, suggesting that their combination may result in a full battery operating in the 3.4 V range. This is in fact the case; see Figure 6B which illustrates the multistep voltage profiles at a C/3 rate (with electrochemical activation of the anode, see the Experimental Section) ranging between 2.3 and 4.2 V and centered at about 3.4 V. A decay of the average discharge voltage is observed in the full lithium ion cell cycling response. This decay may be ascribed to the restoring of the cell-balance upon cycling, which is deeply influenced by the very high specific capacity of the CuO−MCMB anode here adopted. Moreover, it cannot be excluded that the evolution over time of the solid electrolyte interphase affects the electrode kinetics, and, therefore, the operating voltages of the cell.

The battery delivers a specific capacity of about 100 mAh g^{-1} (referred to the cathode mass) with a Coulombic efficiency of about 76% at the first charge−discharge cycle increasing to 95% during the following cycles. Again, we can safely attribute the initial irreversibility to film formation at the cathode side.

Finally, Figure 6C confirms the good performance of the battery that is cycling with good capacity retention and with an efficiency approaching 100%.

3. CONCLUSION

In this paper we discuss and evaluate a copper-doped, high-voltage $Li_{0.85}Ni_{0.46}Cu_{0.1}Mn_{1.49}O_4$ spinel electrode prepared easily by two steps: a coprecipitation, solid-state process. We show that the electrode is characterized by a favorable morphology based on micrometric particle size. The unique morphology we adopted is characterized by well-developed, crystalline, and aggregated microparticles, that considerably reduces the occurrence of side reactions. We show in fact that our electrode can operate at voltages as high as 5.3 V without sign of electrolyte decomposition. We demonstrate that this electrode, when cycled in lithium battery, can deliver a capacity of about 100 mAh g^{-1}, i.e. a value comparable with those of the literature counterparts, with a high capacity retention and high coulombic efficiency over prolonged cycling. By combining the $Li_{0.85}Ni_{0.46}Cu_{0.1}Mn_{1.49}O_4$ cathode with a conversion-type, CuO−MCMB anode, a full lithium ion battery exhibiting good performances in terms of voltage (3.4 V), coulombic

dx.doi.org/10.1021/am500499a | ACS Appl. Mater. Interfaces 2014, 6, 5206−5211

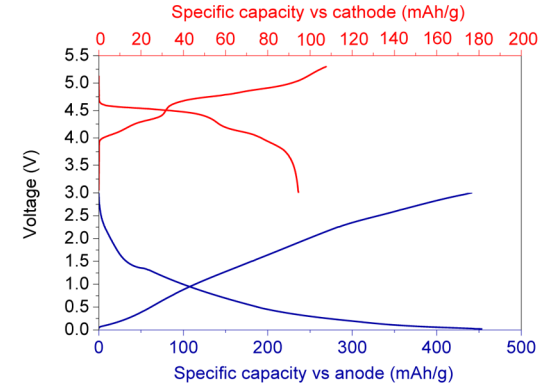

(A)

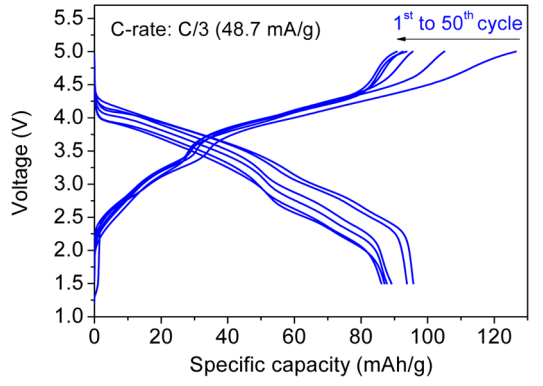

(B)

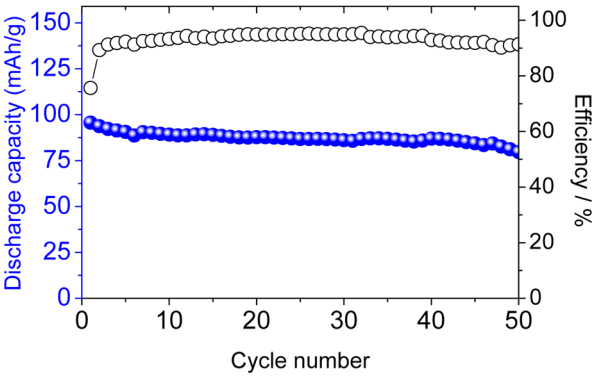

(C)

Figure 6. Typical charge−discharge voltage profiles of the $Li_{0.85}Ni_{0.46}Cu_{0.1}Mn_{1.49}O_4$ cathode and of the CuO−MCMB anode (A), response of the CuO−MCMB/1 M $LiPF_6$ PC/$Li_{0.85}Ni_{0.46}Cu_{0.1}Mn_{1.49}O_4$ lithium ion cell in terms of voltage profiles (B), and capacity versus cycle number at C/3 rate (C).

efficiency (about 95%), and capacity stability for 50 cycles, is obtained. Certainly, further study is required to properly improve the cell configuration, the cycling conditions, including the high temperature setup, and the cell balance. However, to the best of our knowledge, such a copper-based battery system is here originally reported. This battery employs sustainable, eco-compatible, low-cost, and easily prepared electrode materials, an additional bonus that makes it particularly suitable for practical exploitation.

4. EXPERIMENTAL SECTION

Synthesis. The $Li_{0.85}Ni_{0.46}Cu_{0.1}Mn_{1.49}O_4$ sample was prepared by a two-step synthetic route consisting in a coprecipitation followed by a solid state reaction.[25] $NiSO_4·6H_2O$ (Sigma Aldrich, ACS reagent 99%), $CuSO_4·5H_2O$ (Sigma Aldrich, ACS reagent ≥98%), and $MnSO_4·1H_2O$ (Sigma Aldrich, ACS reagent ≥98%) were used as starting materials in the coprecipitation reaction. An aqueous solution of NaOH with a concentration of 4.8 mol/L was continuously added to a 2.4 mol/L aqueous solution of the starting materials in the stoichiometric ratio $NiSO_4·6H_2O$:$CuSO_4·5H_2O$:$MnSO_4·1H_2O$ = 0.225:0.05:0.725. An aqueous solution of NH_4OH was used as chelating agent and added to the solution.

Upon $NaOH_{(aq)}$ dropwise addition, the pH, temperature and stirring speed of the starting materials solution were carefully controlled and set to 11, 25 °C, and 300 rpm, respectively.

The $[Ni_{0.225}Cu_{0.05}Mn_{0.725}](OH)_2$ precursor powder, obtained through the filtration of the solution, was washed with distilled water several times and then dried at 100 °C overnight.

The $[Ni_{0.225}Cu_{0.05}Mn_{0.725}](OH)_2$ powder was then mixed with $LiOH·1H_2O$ (Sigma Aldrich, ACS reagent ≥98%) in the molar ratio $[Ni_{0.225}Cu_{0.05}Mn_{0.725}](OH)_2$:LiOH = 1:2.2 for the synthesis of $Li_{0.85}Ni_{0.46}Cu_{0.1}Mn_{1.49}O_4$. The hydroxide powder was grinded and then annealed in air at 850 °C for 20 h. The composition of the synthesized oxide was determined by inductively coupled plasma−atomic emission spectroscopy (ICP-AES) by using a Vista MPX Rad−VARIAN instrument.

Structural and Morphological Characterization. XRD measurements were performed using a Rigaku D-Max diffractometer equipped with a Cu Kα radiation source. The sample morphology was investigated by scanning electron microscopy using a Phenom-FEI instrument.

Electrochemical Characterization. The $Li_{0.85}Ni_{0.46}Cu_{0.1}Mn_{1.49}O_4$ electrode was prepared by mixing the active material, polivinylidene fluoride PVdF 6020 (Solef Solvay) binder and Super P carbon (MMM Belgium) in the weight ratio (%) 80:10:10, using *N*-methyl-2-pyrrolidone as solvent.

The obtained slurry was cast as thin film on aluminum foils by doctor-blade deposition. The loading of the electrodes was of about 3.5 mg/cm^2.

Swagelok t-type lithium half cells were assembled using a lithium metal foil counter electrode and a Whatman separator soaked in 1 M $LiPF_6$ propylene carbonate (PC) electrolyte solution. The lithium half cells were cycled at different C-rates in the 3−5.3 V vs Li^+/Li voltage range.

The lithium ion full cell was set together by coupling the CuO−MCMB composite film anode[24] with the film cathode in a 1 M $LiPF_6$, PC electrolyte solution. Prior to the cell testing, the CuO−MCMB electrode was electrochemically activated by 2 cycles in a lithium metal cell in the 0.02−3 V vs Li^+/Li voltage range, in order to place it in its steady state working condition.

The specific capacity of the anode was balanced by selecting 1:1 weight ratio versus the cathode with active material loading of 4 mg/cm^2. The lithium ion cell was cycled at C/3 rate, referred to the cathode active material mass, in the 1.5−5 V vs Li^+/Li voltage range.

All the galvanostatic cycling tests of the lithium and lithium ion cells were performed using a Maccor 4000 series Battery Test System. A Bistat Bilogic Science Instrument was used for potentiodynamic cycling with galvanostatic acceleration (PCGA) tests on lithium metal half cells with three-electrode configuration, i.e. by using a lithium metal reference electrode. electrochemical impedance spectroscopy (EIS) tests were run on a Li/1 M $LiPF_6$, PC/$Li_{0.85}Ni_{0.46}Cu_{0.1}Mn_{1.49}O_4$ cell with a Bistat Bilogic Science Instrument, applying a 20 mV amplitude signal in the 1 MHz to 10 Hz frequency range. All the cells were assembled under inert conditions in an argon-filled glovebox, and all the electrochemical tests were performed at room temperature.

AUTHOR INFORMATION

Corresponding Author

*E-mail: jusef.hassoun@uniroma1.it.

Notes

The authors declare no competing financial interest.

■ ACKNOWLEDGMENTS

This work has been supported by the Italian Institute of Technology (Project "REALIST" *Rechargeable, advanced, nano structured lithium batteries with high energy storage*), by "Regione Lazio", Italy, by the Human Resources Development program (No. 20124010203310) of the Korea Institute of Energy Technology Evaluation and Planning (KETEP) grant funded by the Korea government Ministry of Knowledge Economy, and by the National Research Foundation of Korea (NRF) grant funded by the Korea government (MEST) (No. 2009-0092780).

■ REFERENCES

(1) Scrosati, B.; Hassoun, J.; Sun, Y. K. A Look into the Future. *Energy Environ. Sci.* **2011**, *4*, 3287−3295.
(2) Choi, N. S.; Chen, Z.; Freunberger, S. A.; Ji, X.; Sun, Y. K.; Amine, K.; Yushin, G.; Nazar, L. F.; Cho, J.; Bruce, P. Challenges Facing Lithium Batteries and Electrical Double-Layer Capacitors. *Angew. Chem. Int. Ed* **2004**, *51*, 9994−10024.
(3) Scrosati, B.; Garche, J. Lithium Batteries: Status, Perspectives and Future. *J. Power Sources* **2010**, *195*, 2419−2430.
(4) Ellis, B. L.; Lee, K. T.; Nazar, L. F. Positive Electrode Materials for Li-Ion and Li-Batteries. *Chem. Mater.* **2010**, *22*, 691−714.
(5) Winter, M.; Besenhard, J. O.; Spahr, M. E.; Novak, P. Insertion Electrode Materials for Rechargeable Lithium Batteries. *Adv. Mater.* **1998**, *10*, 725−763.
(6) Fergus, J. W. Recent Developments in Cathode Materials for Lithium Ion Batteries. *J. Power Sources* **2010**, *4*, 939−954.
(7) Zhong, Q.; Bonakdarpour, A.; Zhang, M.; Gao, Y.; Dahn, J. R. Synthesis and Electrochemistry of $LiNi_xMn_{2-x}O_4$. *J. Electrochem. Soc.* **1997**, *144*, 205−213.
(8) Santhanam, R.; Rambabu, B. Research progress in high voltage spinel $LiNi_{0.5}Mn_{1.5}O_4$ material. *J. Power Sources* **2010**, *195*, 5442−5451.
(9) Liu, G. Q.; Wen, L.; Liu, Y. M. Spinel $LiNi_{0.5}Mn1.5O_4$ and its Derivatives as Cathodes for High-Voltage Li-ion Batteries. *J. Solid State Electrochem.* **2010**, *14*, 2191−2202.
(10) Hu, M.; Pang, X.; Zhou, Z. Recent Progress in High-Voltage Lithium Ion Batteries. *J. Power Sources* **2013**, *237*, 229−242.
(11) Caballero, A.; Cruz, M.; Hernàn, L.; Melero, M.; Morales, J.; Rodriguez Castillòn, E. Oxygen Deficiency as the Origin of the Disparate Behavior of $LiM_{0.5}Mn_{1.5}O_4$ (M═Ni, Cu) Nanospinels in Lithium Cells. *J. Electrochem. Soc.* **2005**, *152*, A552−A559.
(12) Ein-Eli, Y.; Vaughey, J. T.; Thackeray, M. M.; Mukerjee, S.; Yaug, X. Q.; Mc Breen, J. $LiNi_xCu_{0.5-x}Mn_{1.5}O_4$ Spinel Electrodes, Superior High Potential Cathode Materials for Li Batteries: I. Electrochemical and Structural Studies. *J. Electrochem. Soc.* **1999**, *146*, 908−913.
(13) Liu, J.; Manthiram, A. Understanding the Improved Electrochemical Performances of Fe-Substituted 5 V Spinel Cathode $LiMn_{1.5}Ni_{0.5}O_4$. *J. Phys. Chem. C* **2009**, *113*, 15073−15079.
(14) Wang, H.; Tan, T. A.; Yang, P.; Lai, M. O.; Lu, L. High-Rate Performances of the Ru-Doped Spinel $LiNi_{0.5}Mn_{1.5}O_4$: Effects of Doping and Particle Size. *J. Phys. Chem. C* **2011**, *115*, 6102−6110.
(15) Bruce, P. G.; Scrosati, B.; Tarascon, J. M. Nanomaterials for Rechargeable Lithium Batteries. *Angew. Chemie Int. Ed.* **2008**, *47*, 2930−2946.
(16) Hwang, B. J.; Wu, Y. W.; Venkateswarlu, M.; Cheng, M. Y.; Santhanam, R. Influence of Synthesis Conditions on Electrochemical Properties of High-Voltage $Li_{1.02}Ni_{0.5}Mn_{1.5}O_4$ Spinel Cathode Material. *J. Power Sources* **2009**, *193*, 828−833.
(17) Fan, Y.; Wang, J.; Ye, X.; Zhang, J. Physical Properties and Electrochemical Performance of $LiNi_{0.5}Mn_{1.5}O_4$ Cathode Material Prepared by a Coprecipitation Method. *Mater. Chem. Phys.* **2007**, *103*, 19−23.
(18) Fey, G.T-K.; Lu, C.-Z.; Kumar, T. P. Preparation and Electrochemical Properties of High-voltage Cathode Materials, $LiM_yNi_{0.5-y}Mn_{1.5}O_4$ (M═Fe, Cu, Al, Mg; y=0.0−0.4). *J. Power Sources* **2003**, *115*, 332−345.
(19) Chemelewski, K. R.; Manthiram, A. Origin of Site Disorder and Oxygen Nonstoichiometry in $LiMn_{1.5}Ni_{0.5-x}M_xO_4$ (M═Cu and Zn) Cathodes with Divalent Dopant Ions. *J. Phys. Chem. C* **2013**, *117*, 12465−12471.
(20) Ein-Eli, Y.; Howard, W. F.; Lu, S. H.; Mukerjee, S.; McBreen, J.; Vaughey, J. T.; Thackeray, M. M. $LiMn_{2-x}Cu_xO_4$ Spinels ($0.1 \leq x \leq 0.5$): A New Class of 5V Cathode Materials for Li Batteries. *J. Electrochem. Soc.* **1998**, *145*, 1238−1244.
(21) Scrosati, B.; Abraham, K. M.; Van Schalkwijk, W.; Hassoun, J. *Lithium Batteries−Advanced Technologies and Applications*; Wiley: New York, 2013.
(22) Aurbach, D.; Markovsky, B.; Talyossef, Y.; Salitra, G.; Kim, H. J.; Choi, S. Studies of Cycling Behavior, Ageing, and Interfacial Reactions of $LiNi_{0.5}Mn_{1.5}O_4$ and Carbon Electrodes for Lithium-Ion 5-V cells. *J. Power Sources* **2006**, *162*, 780−789.
(23) Aurbach, D. Review of Selected Electrode−solution Interactions which determine the Performance of Li and Li Ion Batteries. *J. Power Sources* **2000**, *89*, 206−218.
(24) Verrelli, R.; Hassoun, J.; Farkas, A.; Jacob, T.; Scrosati, B. A New, High Performance CuO/ $LiNi_{0.5}Mn_{1.5}O_4$ Lithium-ion Battery. *J. Mater. Chem.* **2013**, *1*, 15329−15333.
(25) Hassoun, J.; Lee, K. S.; Sun, Y. K.; Scrosati, B. An Advanced Lithium Ion Battery Based on High Performance Electrode Materials. *J. Am. Chem. Soc.* **2011**, *133*, 3139−3143.